



(RESEARCH ARTICLE)



A simulated study on the performance evaluation of amorphous silicon solar PV module for temperature, irradiance and tilt angle dependence

VP Sethi *

Department of Mechanical Engineering, Punjab Agricultural University, Ludhiana-141004, India.

Global Journal of Engineering and Technology Advances, 2023, 14(02), 008–029

Publication history: Received on 01 December 2022; revised on 12 January 2023; accepted on 15 January 2023

Article DOI: <https://doi.org/10.30574/gjeta.2023.14.2.0013>

Abstract

The performance of an amorphous silicon solar PV module is tested at various irradiance levels, operation temperatures and tilt angles using a solar simulator. Electrical efficiency, V-I characteristics and power conditioning curves are generated at various solar irradiance levels of 400, 700 and 1000 W/m², cell operation temperature range of 40 to 100°C and various panel tilt angles of 0°, 15°, 30°, 45° and 60° with horizontal. Solar equations are used to compute the maximum swing angle of the sun away from the normal position of the panel at noon (λ) during different months and latitudes. Analogy between the simulated study and λ (for real operation conditions) for polar mounted inclinations of PV panels, winter & summer maximization inclinations of the PV panels and south facing vertical walls/windows for different months of the year and at various latitudes is established and the effect of λ on the percent reduction in maximum power produced (P_{mp}) by the PV solar panel is studied. The tilt angle dependence shows that the panel produces highest P_{mp} at $\lambda = 0^\circ$ (tilt angle of the panel when the light source is normal to the panel surface). It is also observed that P_{mp} decreases by about 9%, 14 % and 19% when λ is 15°, 30° and 45° respectively as compared to the normal position of the panel. Newton-Raphson's technique is used to theoretically compute I_{mp}, V_{mp} & P_{mp} and compared with the experimental values generated using the solar simulator within less than 5% deviation.

Keywords: Photovoltaic; Solar cells; Simulated studies; Tilt angle; Solar Irradiance; Swing angle of the sun

1. Introduction

The cleanest source of 21st century is photovoltaic power generation systems. The technological advancement of this technology has grown tremendously in terms of performance, stability and reliability as several types of solar cell materials have shown great promise with different uses such as; electricity generation, water pumping and lighting using solar panels etc.

Out of available type's crystalline silicon (c-Si) and polycrystalline silicon (poly-Si) solar cell modules are generally used for power generation systems due to higher conversion efficiency. Apart from these, research on thin film solar cell modules consisting of hydrogenated amorphous silicon (a-Si:H) for power generation systems is also on advanced stage.

It is known that available PV panel area exposed to the sun generates the power for small and large scale applications during an hour or a day. Although manufacturers provide the output characteristics of voltage and current (power) under standard test conditions (STC), for design engineers, the prediction of PV panel performance is utmost essential. However, under real operation conditions in which light intensities as well as large temperature variations take place, the actual performance of PV panels tend to differ from given specifications. It has been observed that, three key factors strongly affect the overall performance of PV panels such as; solar radiation availability, cell temperature and tilt angle of the panel. It is apparent that solar radiation changes accordingly to earth locations, time of the day and seasons.

*Corresponding author: VP Sethi

Three key physical quantities can be determined from the I-V characteristics such as: the short-circuit current (I_{sc}), the open-circuit voltage (V_{oc}) and the maximum power to be obtained which are most important variables and correspond to well defined points in the I-V plane. For the accurate assessment and prediction of appropriate PV cell modules, determination of these points becomes essential. Iterative numerical calculations are also needed due to the nonlinear and implicit relationships that exist between them (Villalva et al., 2009). It is known that with increase of temperature the efficiency of photovoltaic solar cells decreases which eventually shows drop of open circuit cell voltage (Sze, 1981). It has been shown through earlier theoretical studies that the decrease in cell efficiency with increase in temperature is inevitable (Wysocki and Rappaport, 1960). The effects of recombination normally enhance the efficiency variation with temperature. Several subsequent studies present the results of temperature coefficients of solar cells parameters (Green et al., 1982, Osterwald et al., 1987, Nann and Emery, 1992). It has been observed that normally the solar cell is exposed to ambient temperatures varying from 10 to 50°C and V_{oc} decreases where as I_{sc} increases slightly with temperature and curve factor (CF) also decreases due to which overall cell efficiency decreases (Friedman, 1996). In order to describe the I-V characteristics of a p-n junction solar cell under steady-state illumination exponential model was used (Priyanka Singh, 2008). Several studies have been conducted in the past to investigate the correct tilt angle or orientation of solar power systems (Lewis, 1987) and greenhouses (Sethi 2009). Empirical or analytical models have been presented by several authors for the computation of the optimum tilt angle (b_{opt}) by relating solar radiation availability models with the collector surface and angle (EL-Kassaby, 1988; Soulayman, 1991; Ibrahim, 1995). The computed models are developed for a specific period of time and purpose showing daily, monthly, seasonal or yearly values. An analytical model based on long-term averaging of solar data was presented by Elsayed (1989) in which it was that recommended the on yearly basis optimum tilt angle is about $\varphi \pm 10^\circ$ (φ : latitude).

Nakamura et al. (2001) used pyranometer to measure the irradiance at six different orientations and three tilt angles to develop correlation between temperature and output power of solar cells and concluded that optimum tilt angle was 30° facing south, i.e. $b_{opt} \sim \varphi$. TRNSYS simulation software was used by Hussein and Ahmad (2004) to simulate a solar power plant using mean monthly global radiation and compared with the output power of solar cells. It was concluded that yearly optimum tilt angle is $\varphi_{opt} = \varphi - 10^\circ$. Reflection losses from cover materials were presented by Balenzategui and Chenlo (2005) by studying the reflection characteristics of the collector surface.

Gunerhan and Hepbasli (2007) conducted a very important study to compute the monthly optimum tilt angles and it was observed the optimum tilt angle was equal to latitude angle (φ) for year round performance, $b_{opt} = \varphi - 15^\circ$ (for summer) and $b_{opt} = \varphi + 15^\circ$ (for winter). Simulation software PVSYST was used by Cheng et al. (2009) of a fixed solar collector and the latitude to develop correlation and concluded that by using optimum tilt angle (the latitude angle) of the panel, 98.5% of full capacity of a solar power plant can be obtained. Kaddoura et al. (2016) discussed the important factors like; sun position, latitude and local geographical characteristics along with tilt angle of photovoltaic (PV) panels for performance evaluation using MATLAB software for maximum solar radiation availability and inferred that by adjusting tilt angles of panels six times in a year can capture about 99.5% of the solar radiation. Ruidong et al. (2017) developed a correlation of tilt angle and dust deposition with output power of PV panel by analyzing the Hay, Davies, Klucher, Reindl (HDKR) solar radiation model using MATLAB software. Jacobson and Vijaysinh (2018) used 3rd order polynomial fit of optimal tilt angle of PV panel and latitude at global level and analysis was conducted using global 3-D GATOR-GCMOM model which was one-axis vertically tracked, one-axis horizontally tracked.

Ullah et al. (2019) developed a model for the optimal PV tilt angle and conducted experiments for various PV tilt angles for validation of the model. Results showed that from 10% to 40% of power loss could occur due to lighter or heavier soiling of the panel. Meng et al. (2020) studied the orientation (i.e. tilt and azimuth angles) of PV modules for their performance studies using curve-matching procedure in which PV power generation data and off-site irradiance data at an interval of one hour was used. The developed method could accurately parameterize azimuth and tilt angles of PV panels. Yadav and Panda (2020) conducted studies for optimally tilted semi-transparent BIPV panel fixed on the roof of a two-storied single room sample building and evaluated the thermal performance by developing energy equilibrium differential equations. It was observed that the efficiency of the BIPV panel reduced by 18% with the increase in cell temperature to 65 °C as compared to standard test condition.

Mamun et al. (2021) discussed the performance of Photovoltaic (PV) system's performance as affected by orientation and tilt angle and conducted experimental studies to find out the PV panel performance variation and electrical parameters at different tilt angles. Two experimental modes were used; at 750 W/m² and module tilt angle variation from 0° to 80° using a single-axis tracker. It was observed that with every 5° increase in tilt angle causes a power drop of 2.09 W at under constant irradiation of 750 W/m² at indoor and 3.45 W at outdoor. Abdulmunem (2021) discussed the effect of tilt angle on the amount of solar radiation received and presented specific to PV/PCM system, in which PCM was used as passive cooling method for the PV cells. Various tilt angles (0°, 30°, 60°, and 90°) were used and the results

presented that the melting process time of PCM decreased as the tilt-angle of PV/PCM system increased from 0° to 90°, resulting in overall PV cell temperature drop from -0.4% to -12%.

From the literature review it is clear that the solar cell/panel output depends mainly upon three parameters such as; solar irradiance, operation temperature and tilt angle. The previous studies performed to evaluate the performance of solar cells/panels, only one or two parameters out of the above mentioned three parameters have been studied. In the present study, a solar simulator is developed and used to experimentally test a solar module (15 watt peak, 12 V, amorphous silicon solar panel used for battery charging) at various irradiance levels (400, 700 and 1000 W/m²), operation temperatures (40 to 100°C) and tilt angles (0, 15, 30, 45 and 60° with horizontal). The electrical efficiency, V-I characteristics, power conditioning curves at each selected parameter are generated experimentally. Mathematical expressions using Newton-Raphson’s method have been used to theoretically compute I_{mp} , V_{mp} and ultimately P_{mp} and compared with the experimental values generated using a solar simulator.

2. Theoretical aspects

The effect of operating temperature on the electrical efficiency of a PV cell/module can be traced to the temperature’s influence upon the current I, and the voltage V, as the maximum power is given by

$$P_{mp} = V_{mp} I_{mp} = (FF) V_{oc} I_{sc} \dots\dots\dots(1)$$

In this fundamental expression, which also serves as a definition of the fill factor (FF), subscript m refers to the maximum power point in the module’s I–V curve, while subscripts oc and sc denote open circuit and short circuit values, respectively. It turns out that both the open circuit voltage and the fill factor decrease substantially with temperature (as the thermally excited electrons begin to dominate the electrical properties of the semi-conductor), while the short circuit current increases, but only slightly for c-Si solar cells (Zondag, 2007). This study is aimed at quantifying the effect of operation temperature for an amorphous silicon solar module.

2.1. Electrical efficiency

A linear relation as suggested by Skoplaki and Palyvos, 2009 is used for computing electrical efficiency (η_c)

$$\eta_c = \eta_{T_{ref}} [1 - \beta_{ref} (T_c - T_{ref}) + \gamma \log_{10} G_T] \dots\dots\dots(2a)$$

In which $\eta_{T_{ref}}$ is the module’s electrical efficiency at the reference temperature, T_{ref} , and at solar radiation flux of 1000 W/m² (G_T). The quantities $\eta_{T_{ref}}$ and β_{ref} are normally given by the PV manufacturer. In the current study these values are taken as 0.05 and 0.011 for amorphous silicon. If the efficiency is to be taken at one sun then the Eq. 2a is changed to Eq. 2b as suggested by Skoplaki and Palyvos, 2009

$$\eta_c = \eta_{T_{ref}} [1 - \beta_{ref} (T_c - T_{ref})] \dots\dots\dots(2b)$$

2.2. V-I characteristics and maximum power output

From the measured solar cell parameters (I_{sc} , V_{oc} , T_c) the maximum power (P_{mp}) can be calculated. The maximum power of a solar cell is the point on the V-I characteristic curve, at which the product $P = I \times V$ is at its maximum value. The relation between I and V for an illuminated solar cell is given by the following Eq. (Wagner, 2006);

$$I = I_{il} - I_0 \left(e^{\frac{V + IR_s}{V_T}} - 1 \right) \dots\dots\dots(3)$$

Or expressed by V

$$V = V_T \times \ln \left(\frac{I_{il} - I + I_0}{I_0} \right) - I R_s \dots\dots\dots(4)$$

V_T was calculated from the measured temperatures (T_c) by using the formula;

$$V_T = \frac{mkT_c}{q} \dots\dots\dots(5)$$

Values of the *mare* in the range of 1 and 2. A value of $m = 1.6$ was chosen for this study. The diode current (I_0) was determined from the measured open circuit voltage by employing the expression (Wagner, 2006);

$$I_0 = I_{il} e^{-\frac{V_{oc}}{V_T}} \dots\dots\dots(6)$$

R_s was assumed to be 0.03Ω , which is a commonly used value in literature. Neglecting the resistance and with $V = 0$ it follows from Eq. (7) (short circuit) that $I_{il} \sim I_{sc}$. To compute P_{mp} , a computer program was developed using Newton-Raphson’s iterative method. After some rearrangements and substitutions in Eq. (3) and Eq. (4), the following Eq. (7) is obtained.

$$I_{mp} + \frac{(I_{mp} - I_{sc} - I_0) \left[\ln \left(\frac{I_{sc} - I_{mp}}{I_0} + 1 \right) - \frac{I_{mp} R_s}{V_T} \right]}{1 + (I_{sc} - I_{mp} + I_0) \frac{R_s}{V_T}} = 0 \dots\dots\dots(7)$$

I_{mp} denotes the electric current at its maximum point. Application of Newton-Raphson’s method on the previous expression yields

$$I_{mp_{i+1}} = I_{mp_i} - \frac{f(I_{mp_i})}{f'(I_{mp_i})} \dots\dots\dots(8)$$

The subscript i denotes the i th iteration. $f(I_{mp_i})$ is denoted in Eq. (9) and its derivative $f'(I_{mp_i})$ in Eq. (10) respectively.

$$f(I_{mp_i}) = I_{mp_i} + 2(I_{sc} + I_o - I_{mp_i}) I_{mp_i} \frac{R_s}{V_T} + (I_{mp_i} - I_{sc} - I_o) [\ln(I_{sc} + I_o - I_{mp_i}) - \ln(I_o)] = 0 \dots\dots\dots(9)$$

$$f'(I_{mp_i}) = 2(1 - 2I_{mp_i} \frac{R_s}{V_T}) + 2(I_{sc} + I_o) \frac{R_s}{V_T} + [\ln(I_{sc} + I_o - I_{mp_i}) - \ln(I_o)] \dots\dots\dots(10)$$

Using iterative method of Eq. 8, I_{mp} is determined. Thereafter, V_{mp} and P_{mp} can be calculated using Eq. (11) and Eq. (12) respectively.

$$V_{mp} = V_T \ln \left(\frac{I_{sc} - I_{mp}}{I_0} + 1 \right) - I_{mp} R_s \dots\dots\dots(11)$$

$$P_{mp} = I_{mp} \times V_{mp} \dots\dots\dots(12)$$

2.3. Temperature dependence of power output

An empirical expression for amorphous silicon PV panel power output as a function of temperature (Yamawaki et al., 2001) is also used for computing the power.

$$P_{mp} = P_{25} [1 - 0.0026(T_c - 25)] \dots\dots\dots(13)$$

This maximum power output is compared with the P_{mp} obtained through Eq. (12) using the Newtons-Rapson’s method and the experimentally observed values using simulated study.

2.4. Tilt angle dependence on maximum power produced of the PV panel

It is known that the maximum power is produced by a PV panel when the sun rays strike its plane at normal (perpendicular) position. To keep the sun rays at the normal position during the sunshine hours, 2-axis sun trackers are used, but they add to the cost of the already expensive PV systems for electricity generation. Although maximum power point trackers (MPPT) can also be used to obtain maximum power on any given V-I characteristics curve generated when the sun rays are not necessarily at normal position to the PV plane. The dependence of tilt angle of the panel on the maximum power output depicts the percentage reduction in maximum power produced when the sun rays are not in normal position to the module plane.

It is known that at any latitude, solar irradiance incident on the module is maximum around the noon hours which, in turn helps in producing the maximum power output from it. In this study, horizontal placement of the PV panel in a simulator means normal position of the sun rays to the module plane during noon hours. Similarly, 15° tilt angle of the panel means the situation when the sun rays are directed at 15° away from the normal position during noon hours and so on as shown in Fig. 1(a). Simulated study at various tilt angles can be related to the real operating situations when the maximum solar altitude angle of the sun with horizontal (α_s) does not reach at the normal position of the panel at various latitudes as shown in Fig 1(b). The maximum altitude angles of the sun at noon hours during different months of the year at selected latitudes were computed using solar equations as shown in Table 1. These data is then used to compute the maximum swing angle of sun away from the normal position of the panel (λ) in degrees ($\lambda=0$ when sunrays are normal to the module plane). It is known that any inclination away from the normal (to the sun rays) would lead to the reduction in the maximum power produced by the PV panel. From the simulated study of the tilt angle dependence on the maximum power output, the percent reduction in the maximum power produced is thus computed and discussed in the results for different months of the year at various selected latitudes. This study is aimed at quantifying the percent reduction in maximum power produced with respect to increase in λ at various irradiance levels and at different latitudes.

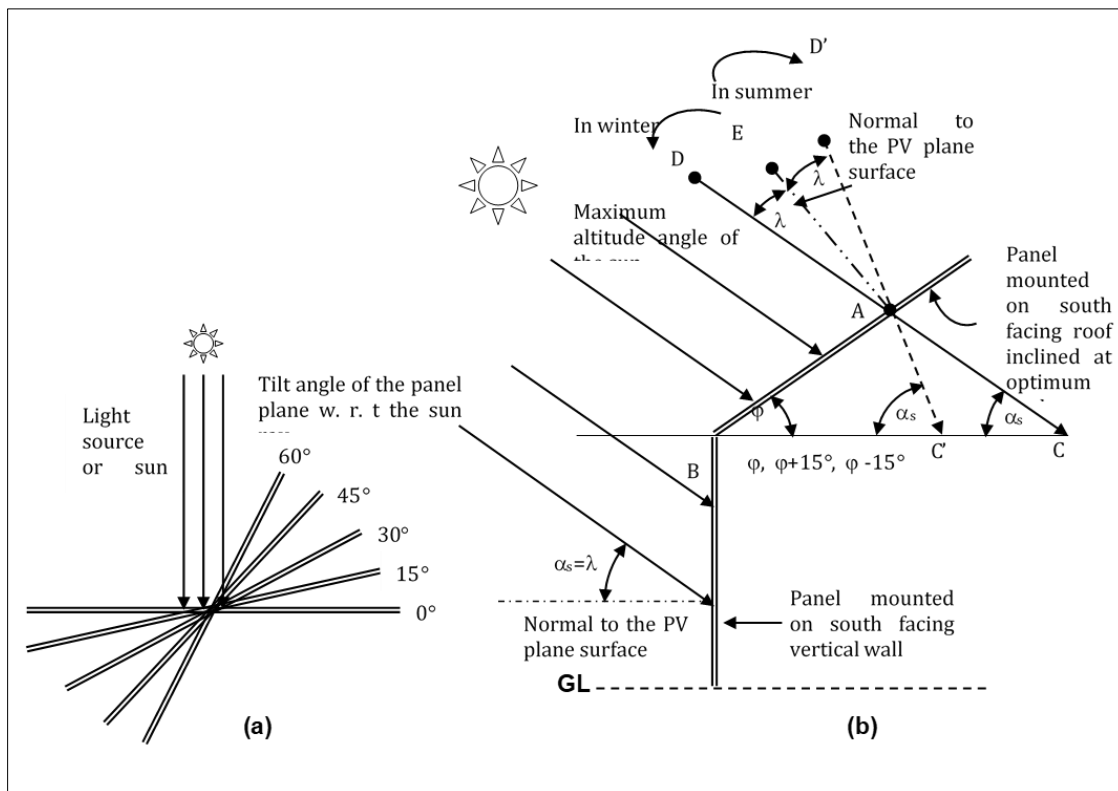


Figure 1 The analogy of simulated conditions (a) with the real conditions (b) to compute the maximum power produced as a function of swing angle of the sun away from the normal position at solar noon

2.4.1. Maximum swing angle of the sun away from the normal for (a) polar mounted and (b) winter & summer maximization inclinations of the panel

Fig 1(b) shows the optimum inclination of the panel ($\beta_{opt} = \varphi$, polar mounted) on the roof of a building for year round application. It is known that the maximum altitude angle of the sun at noon (α_s) is small during the winter months at any latitude as compared to summer months as shown in Table 1. The variation of α_s in winter months and summer months with respect to the normal of the sun ray position of the panel is also shown in Fig. 1(b). During summer months the sun rays point even away from the normal to the inclined PV plane resulting in drop of maximum power produced.

In $\triangle ABC$

$$\angle BAC = 180^\circ - (\varphi + \alpha_s) \dots\dots\dots (14)$$

$$\angle DAB = 180^\circ - \angle BAC \dots\dots\dots (15)$$

In winter, λ for each month is given as

$$\begin{aligned} \lambda &= 90^\circ - \angle DAB \dots\dots\dots (16) \\ \angle EAB &= 90^\circ \end{aligned}$$

Average swing angle of sun during winter months (in northern hemisphere) is

$$\overline{\lambda}_W = (\lambda_J + \lambda_F + \lambda_M + \lambda_O + \lambda_N + \lambda_D) / 6 \dots\dots\dots(17)$$

In summer

$$\lambda = \angle DAB - 90^\circ$$

Average swing angle of sun during summer months (in northern hemisphere) is

$$\overline{\lambda}_S = (\lambda_A + \lambda_M + \lambda_J + \lambda_J + \lambda_A + \lambda_S) / 6 \dots\dots\dots(18)$$

Table 1 shows the maximum altitude angle of the sun (with horizontal) at noon (α_s) and the swing angle of sun away from the normal (λ) at various selected latitudes during mid-day of the month (representative value) for polar mounted PV panels ($\beta_{opt} = \varphi$). Table 2 shows the maximum altitude angle of the sun (with horizontal) at noon (α_s) and the swing angle of sun away from the normal (λ) at various selected latitudes during the representative day of each month (15th date) for winter and summer maximized mounted PV panels. ($\beta_{opt} = \varphi + 15^\circ$ for winter months of September, October, November, December, January, February and March and $\beta_{opt} = \varphi - 15^\circ$ for summer months of April, May, June, July, August and September).

Altitude angle of the sun ‘ α_s ’ at any time of the day and for any day of the year can be determined at a specific latitude location is given by Liu & Jordan (1960).

$$\alpha_s = \sin^{-1} (\sin \delta \sin \phi + \cos \delta \cos \phi \cos \omega) \dots\dots\dots (19)$$

Where, ‘ ϕ ’ is the north latitude of location in degrees. ‘ ω ’ is the hour angle in degrees, which is equal to 15° times the number of hours from solar noon. It is negative before noon, zero at noon and positive after 12 noon and is given as

$$\omega = 15 (t_{solar} - 12) \dots\dots\dots (20)$$

Declination angle of the sun in degrees is given by

$$\delta = 23.45 \times \sin [360 (284 + n) / 365] \dots\dots\dots (21)$$

Where, t_{solar} is the local time of the day and n is the day of the year starting from January 1.

Table 1 Variation of maximum altitude angle of the sun and maximum swing angle of the sun at selected latitudes during all months of the year for polar mounted panel inclinations

Month and date	20°N		30°N		40°N		50°N	
	α_s	λ	α_s	λ	α_s	λ	α_s	λ
January 15	48.67	21.33	38.68	21.32	28.68	21.32	18.66	21.34
February 15	56.82	13.18	46.8	13.20	36.80	13.20	26.74	13.26
March 15	67.37	02.63	57.35	02.65	47.30	02.70	37.30	02.70
April 15	79.11	09.11	69.23	09.23	59.20	09.20	49.20	09.20
May 15	87.44	17.44	78.81	18.81	68.91	18.91	58.87	18.87
June 15	86.37	16.37	83.21	23.21	73.13	23.13	63.25	23.25
July 15	87.44	17.44	81.11	21.11	71.26	21.26	61.28	21.28
August 15	83.21	13.21	73.33	13.33	63.38	13.38	53.41	13.41
September 15	71.62	01.02	62.13	02.13	51.72	01.72	41.68	01.68
October 125	59.99	10.01	49.9	10.10	39.94	10.06	29.67	10.33
November 15	47.14	22.86	40.69	19.31	30.66	19.34	20.67	19.33
December 15	46.55	23.45	36.51	23.49	26.49	23.51	16.44	23.56

2.4.2. Maximum swing angle of the sun away from the normal for a solar panel mounted on vertical wall/window facing south

The new developments in the PV thin film solar cell research has also shown that in future these thin films would be fixed on the south facing walls and windows as facades to increase the used area for PV systems and to save the roof and ground space. However, the vertical inclination of the wall (90°) on which these thin films would be used and the maximum altitude angle of the sun with horizontal (α_s) has to be studied along with the maximum swing angle for sun away from the normal of the wall (λ). Fig. 1b also shows the position of a panel on the vertical wall of a building. It is observed that higher altitude angle of the sun (α_s) in summer months on the vertical wall would result in lesser maximum power produced due to greater swing angle of the sun away from the normal. The simulated study is also aimed at quantifying the reduction in maximum power produced by solar PV panels/films mounted/would be mounted on south facing walls of the buildings and the comparative reduction of maximum power produced if the panel is mounted on the wall as compared to the roof. In this situation (of using a solar PV thin film on the vertical window and wall) the altitude angle of the sun becomes equal to the maximum swing of the sun away from the normal

$$\alpha_s = \lambda \dots\dots\dots 22)$$

3. Experimental set up

Testing of solar panel was done in the research laboratory of the Department of Computer Sciences and Electronics, North Dakota State University, Fargo, USA during the month of March 2011. Experimental set up consisted of a solar simulator fitted with two light sources (metal halide HID lamp of one kW each) hung from top of the simulator roof, facing a horizontal platform which was modified to move up and down in the vertical direction (Fig. 2(a) Fig. 2(b) and Fig.2(c) pictorial view) using a steel rope and pulley arrangement. An amorphous silicon solar PV module producing 15 W (maximum power output at standard test conditions) and used as battery charger was placed centrally on the movable platform for testing at various tilt angles (inclined positions) with respect to the light source (Fig. 3a). Stainless steel solid triangles inclined at 0°, 15°, 30°, 45° and 60° angles (with the light source) were fabricated and placed one by one below the panel to test the solar panel at various inclinations. Three variable resistances (rheostats) were used to apply load on the PV module for generating V-I characteristics and power conditioning curves at selected irradiance and operation temperatures (Fig. 3b). In order to control the operation temperature of the PV module, two high speed fans were fitted and operated from below the wired mesh platform on which the PV module was placed for selective cooling of the panel. The irradiance levels falling on the PV module were varied by altering the vertical distance between the light source and the movable platform on which the module was placed. The power, voltage and current output were

recorded at each load using WT 2030 model digital power meter. Cell temperature of the module (surface temperature beneath the glass cover) was recorded using a non-contact type hand held infrared thermometer having operating range of -20° to 320° C. The thermometer was pointed towards the module from 30 cm distance at three different locations on the module and then the average was taken. The sensor of a digital solarimeter (SL-100, KIMO make Italy) was placed on the horizontal surface of the simulator plane for measured the solar radiation (Fig. 3b). Using standard solar equations, solar radiation on an inclined surface (equivalent to the inclination of the module plane) was then computed. Sufficient time was given to the module for attaining a constant operation temperature before recording any data. The ambient temperature conditions in the laboratory were about 25° C.

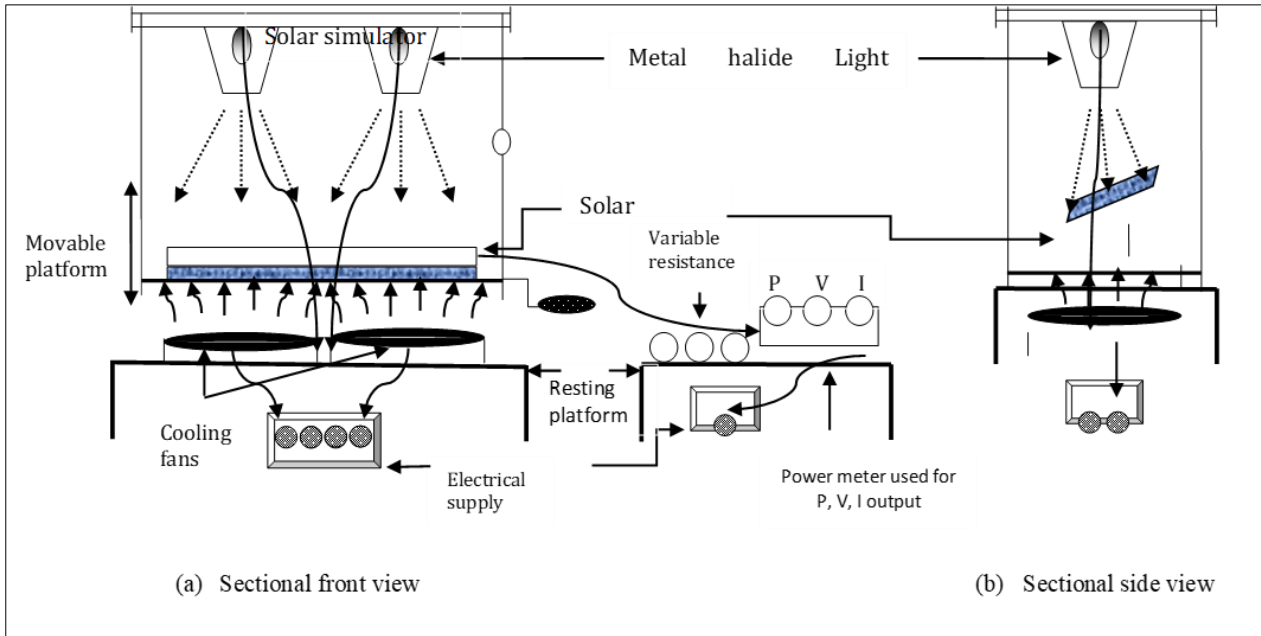


Figure 2 Experimental set up showing sectional front view (a) and sectional side view (b) for testing of solar (PV) module using a solar simulator



Figure 2c Pictorial view of the solar simulator along with apparatus used load circuit while testing of amorphous silicon panel

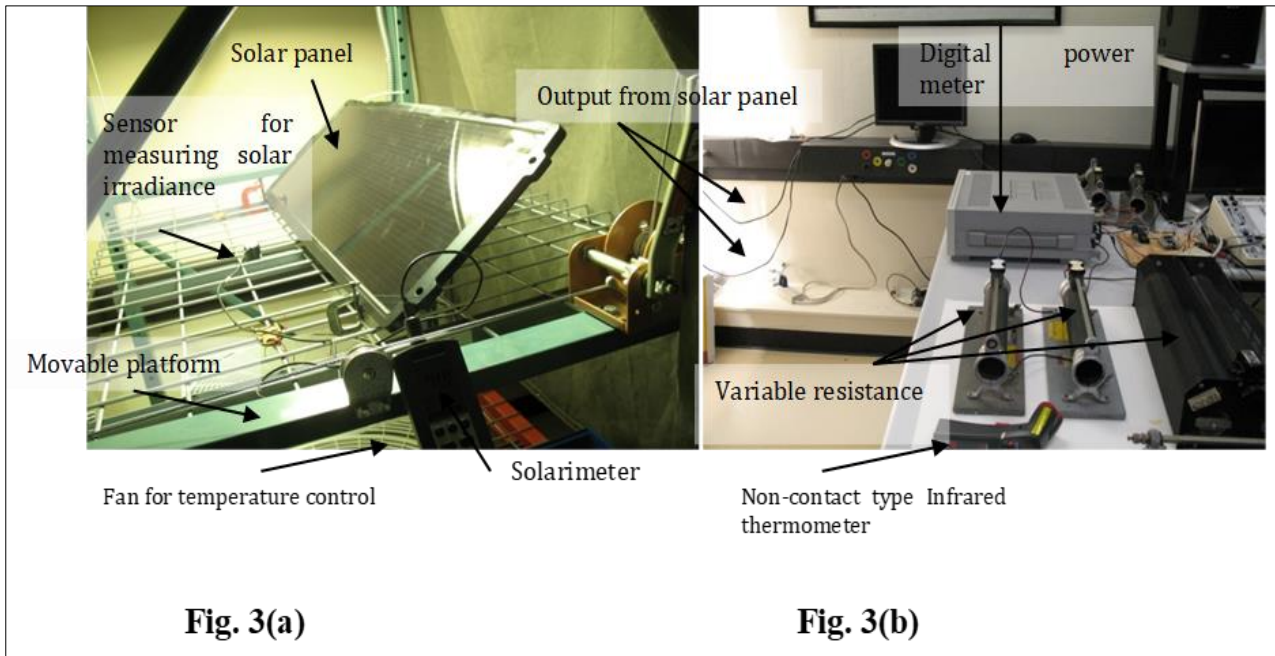


Figure 3(a) Pictorial view of solar simulator being used for panel testing at selected tilt angles and **3(b)** shows the experimental set up to measure the Voltage, current and power output at various loads

4. Results and discussion

4.1. Solar module efficiency as a function of solar irradiance and operating temperature

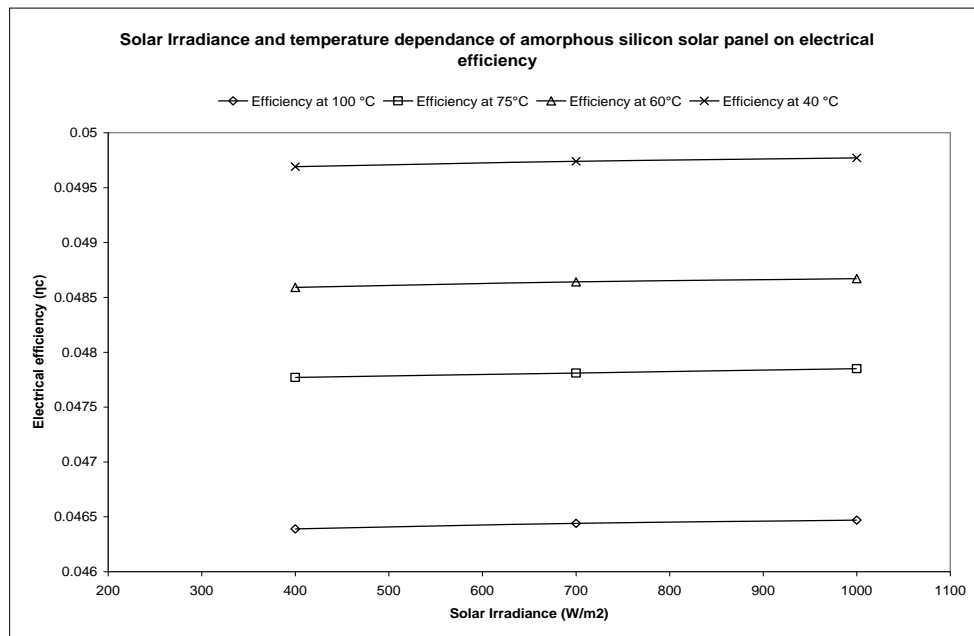


Figure 4 Effect of solar Irradiance and operation temperature on the electrical efficiency of amorphous silicon solar panel

The pronounced effect of solar radiation and operating temperature on the electrical efficiency of the amorphous silicon PV module is computed using Eq. 2a and Eq. 2b and shown in Fig. 4. The solar cell temperature was varied from 40 °C to 100 °C and solar irradiance from 400 W/m² to 1000 W/m². A study by Skoplaki and Palyvos, 2009 suggested that the maximum efficiency of amorphous silicon solar panel cannot be more than 5% at 25°C (STC). Using Eq. 2b, the pronounced effect of operation temperature is computed on the electrical efficiency of the solar module. It was observed

that as the operation temperature decreased, the electrical efficiency of the panel increased. The lowest efficiency was 0.0464 at 100°C and increased to 0.0496 at 40 °C. It was also observed that at the same operation temperature, the electrical efficiency increased with increase in solar irradiance. The measured value of electrical efficiency was also 5 % as the area of the panel was 0.3m² (30 cm × 100 cm) and the W_p shown by the manufacturer were 15 W at 1000 W/m² of solar irradiance.

4.2. I-V characteristics and maximum power produced as a function of solar irradiance and tilt angle

Testing of solar module at various tilt angles of the panel and selected irradiance levels is presented in this section. V-I characteristics and power output curves generated from experimentally measured data is given in Fig. 5, Fig. 6, Fig. 7, Fig 8 and Fig 9. The figures also show the measured values of V_{mp}, I_{mp} and P_{mp}. A mathematical model was also developed using Newton’s-Rapsons iteration method for computing the maximum power output of a PV solar panel. These computed values were compared with the experimental values generated on solar simulator as shown in Fig. 13.

Fig. 5a shows the V-I characteristics at 0° tilt angle of the panel (horizontal position, when sun rays are normal to the module plane) for various irradiance levels. At the maximum power point value (P_{mp}) of the V-I curve, the values of I_{mp} and V_{mp} were 0.936 A and 14.75 V. The corresponding value of P_{mp} on the power conditioning curve was 13.806 W as shown in Fig. 5b. Ideally the panel should produce 15 W_p maximum power output at STC of 25°C (as given by the manufacturer), but due to continuous use of the panel for battery charging purposes over the last five years, the actual maximum power produced decreased. Moreover, the operating temperature is also higher than the STC value (>40°C), resulting in lowering of the maximum power output. At the same irradiance level of 1000 W/m², when the panel was tilted at 15° with horizontal, I_{mp} and V_{mp} decreased (Fig. 6a). The corresponding value of P_{mp} also decreased (Fig. 6b). This drop in P_{mp} was 9.23% as compared to the P_{mp} produced at horizontal position of the panel. When the panel was tilted at 30° and 45° with horizontal, I_{mp} and V_{mp} further decreased (Fig. 7a and Fig. 8a). The corresponding value of P_{mp} was 14.15% lower (Fig. 7b) and 18.95% lower (Fig. 8b) as compared to the P_{mp} produced at horizontal position of the panel. However, when the inclination of the panel was increased to 60° with horizontal, there was significant change in I_{mp}, V_{mp} (Fig. 9a) resulting in much drop in P_{mp} produced (45.29%) (Fig. 9b). This trend in the drop of P_{mp} was almost similar at other irradiance level of 700 W/m² and 400 W/m² as shown through Fig. 5 to Fig. 9. A comparison of power conditioning curves at various tilt angles is also shown in Fig. 10.

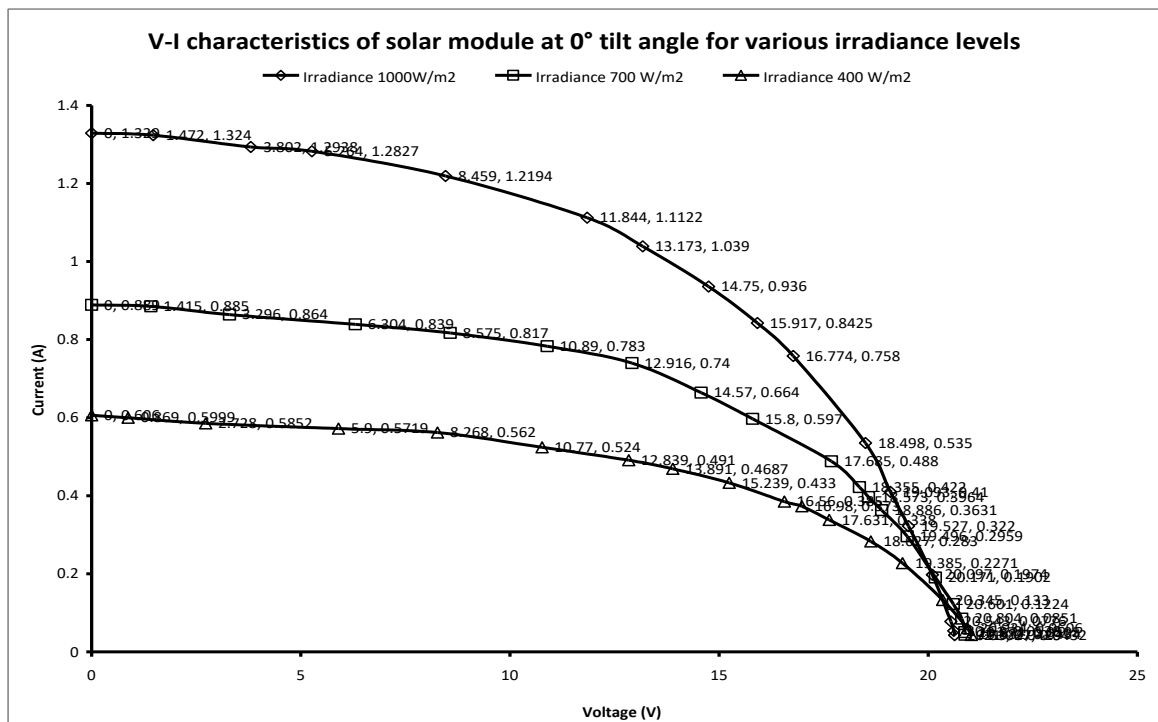


Figure 5a V-I characteristics of solar module at 0° tilt angle (horizontal position with the light source) measured at various solar radiation levels (At 1000 W/m², I_{sc} = 1.3217 A, V_{oc} = 21.14 V), (At 700 W/m², I_{sc} = 0.886 A, V_{oc} = 21.28 V), at 400 W/m², I_{sc} = 0.593 A, V_{oc} = 21.63 V)

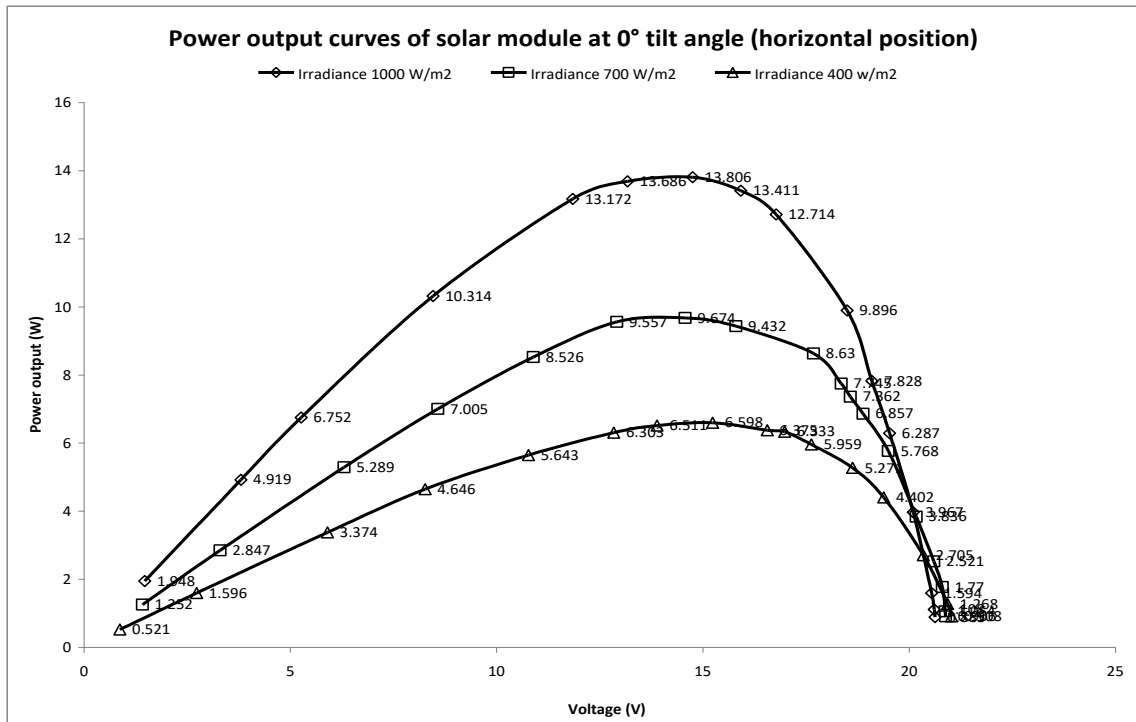


Figure 5b Power output curves of solar module at 0° tilt angle (horizontal position with the light source) measured at various solar radiation levels

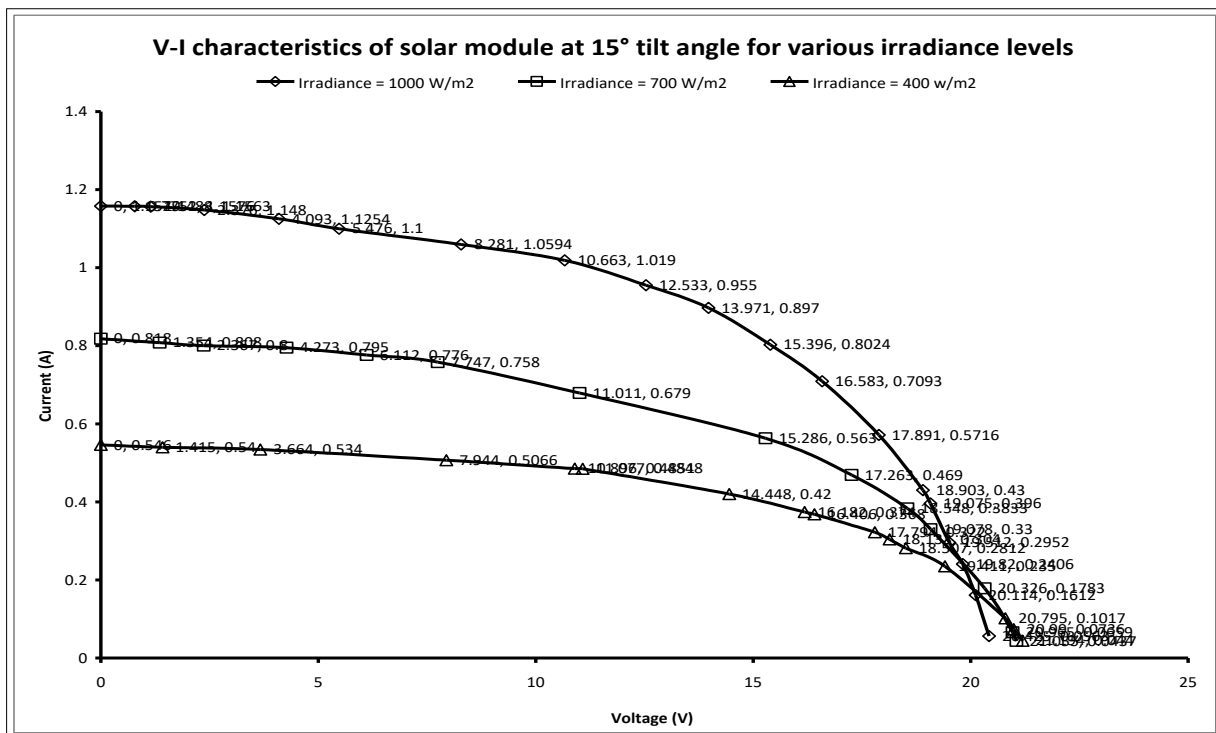


Figure 6a V-I characteristics of solar module at 15° tilt angle (with horizontal) measured at various solar radiation levels. (At 1000 W/m², $I_{sc} = 1.1579$ A, $V_{oc} = 21.57$ V), (At 700 W/m², $I_{sc} = 0.758$ A, $V_{oc} = 21.65$ V), at 400 W/m², $I_{sc} = 0.540$ A, $V_{oc} = 21.73$ V)

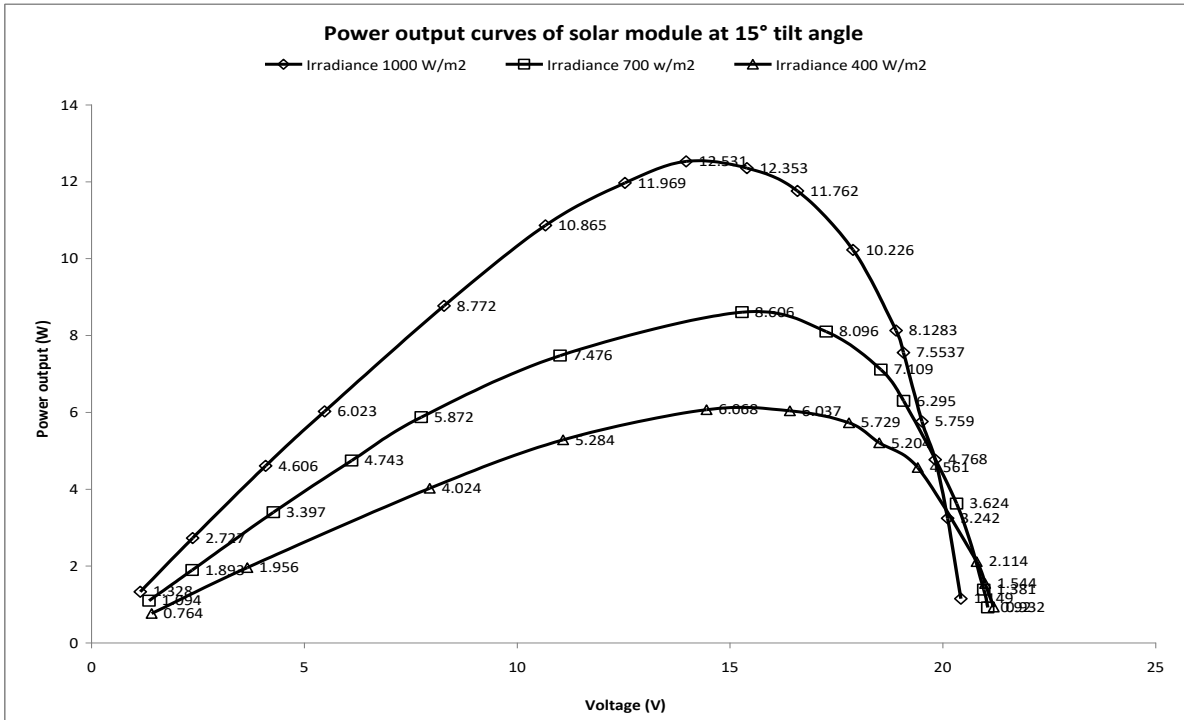


Figure 6b Power output curves of solar module at 15° tilt angle (with horizontal) measured at various solar radiation levels

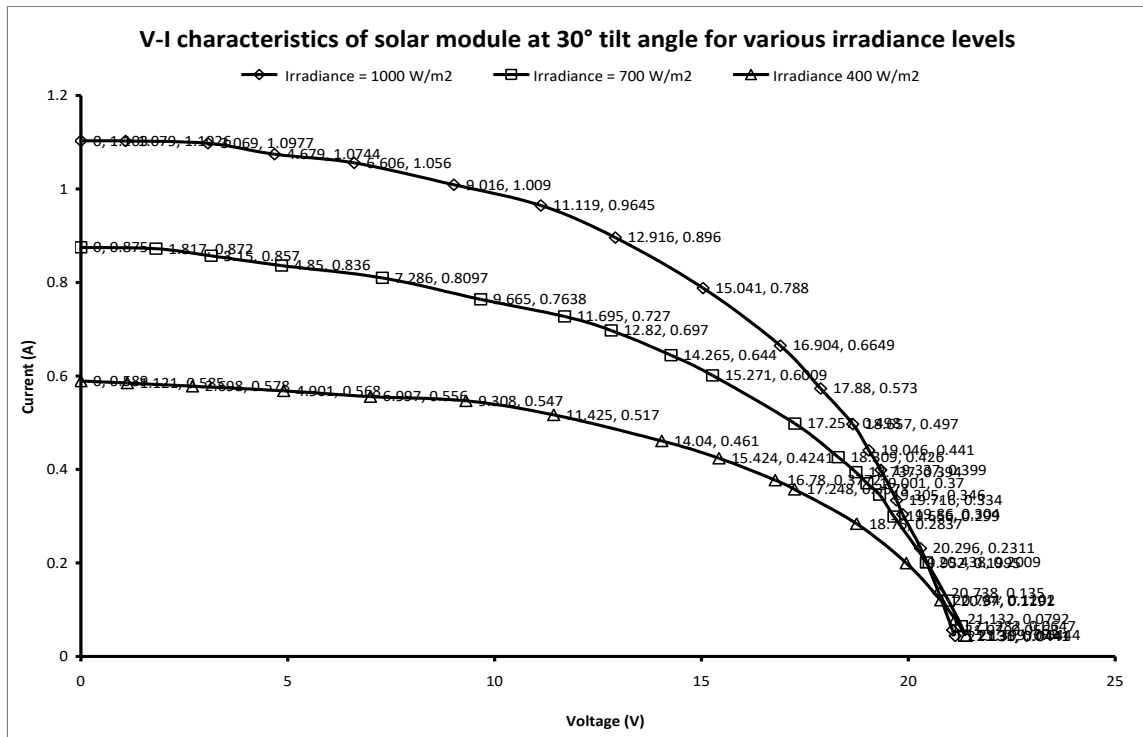


Figure 7a V-I characteristics of solar module at 30° tilt angle (with horizontal) measured at various solar radiation levels. (At 1000 W/m², I_{sc} = 1.10 A, V_{oc} = 21.61 V), (At 700 W/m², I_{sc} = 0.875 A, V_{oc} = 21.91 V), at 400 W/m², I_{sc} = 0.608 A, V_{oc} = 22.00 V)

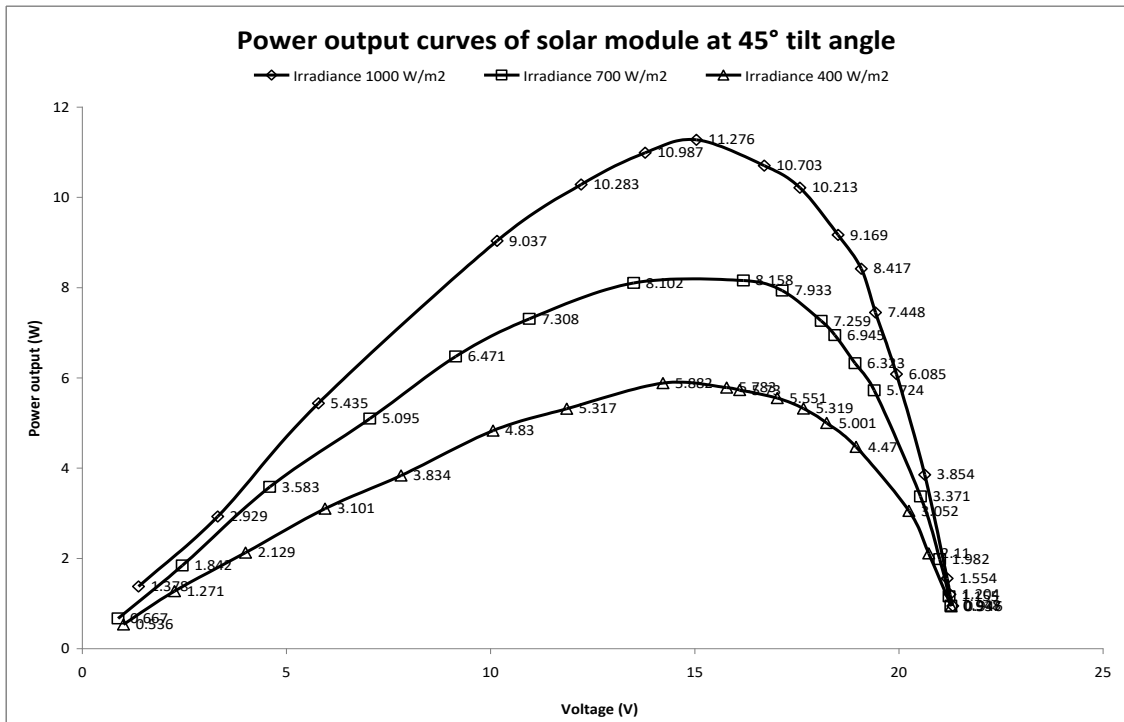


Figure 8b Power output curves of solar module at 45° tilt angle (with horizontal) measured at various solar radiation levels

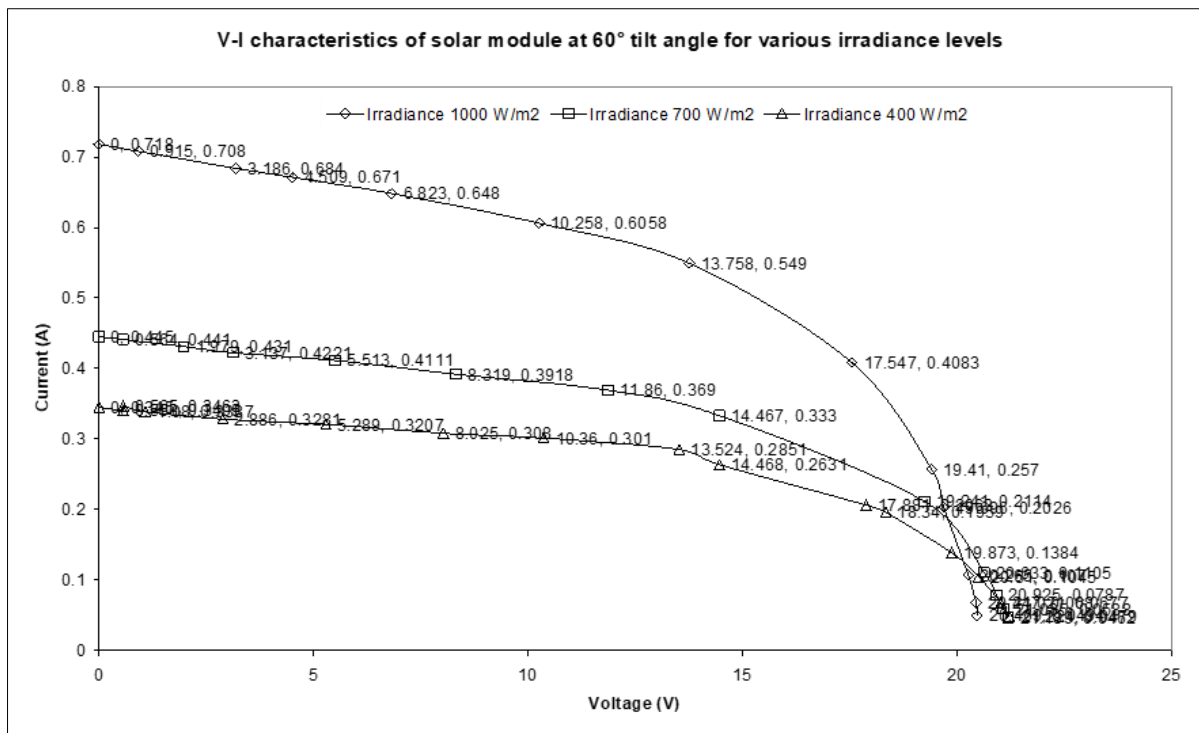


Figure 9a V-I characteristics of solar module at 60° tilt angle (with horizontal) measured at various solar radiation levels. (At 1000 W/m², $I_{sc} = 0.708$ A, $V_{oc} = 20.92$ V), (At 700 W/m², $I_{sc} = 0.441$ A, $V_{oc} = 21.80$ V), at 400 W/m², $I_{sc} = 0.340$ A, $V_{oc} = 21.88$ V)

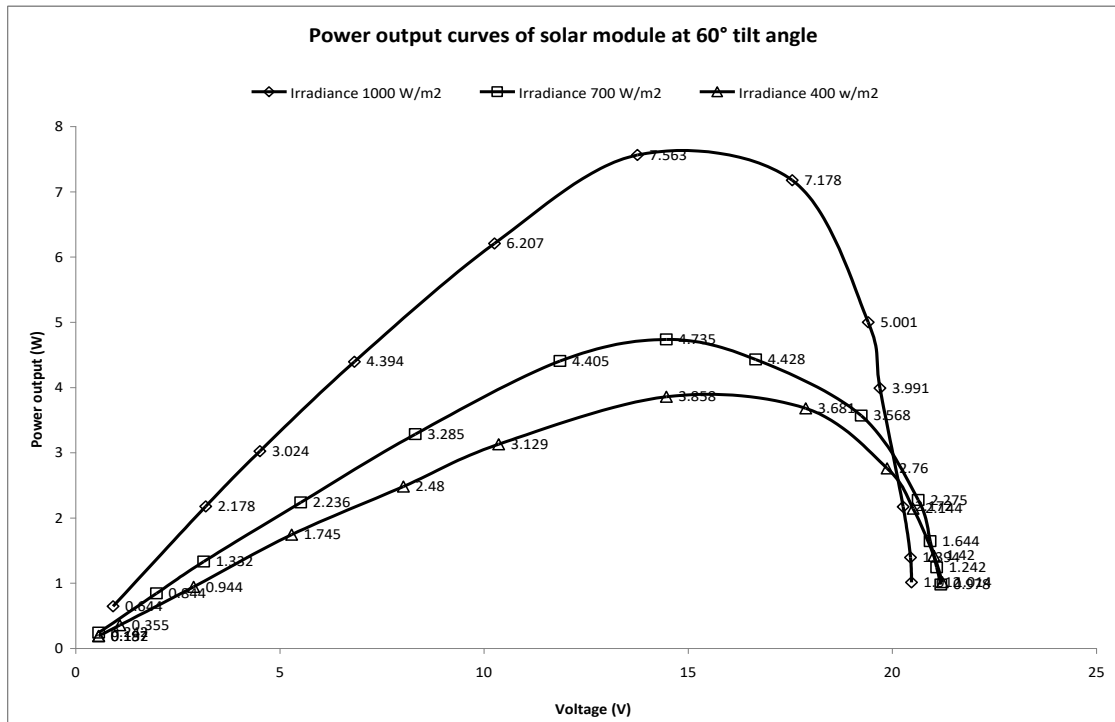


Figure 9b Power output curves of solar module at 60° tilt angle (with horizontal) measured at various solar radiation levels

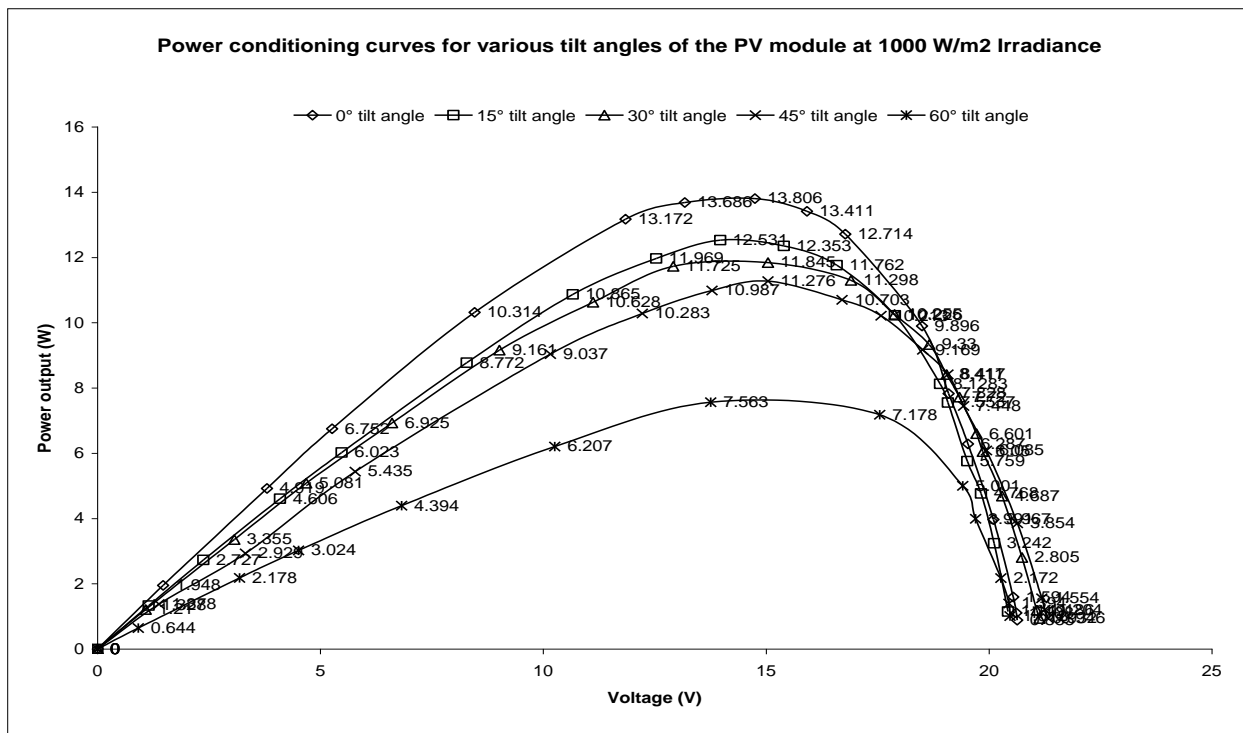


Figure 10 Power conditioning curves showing maximum power output at various tilt angles of the panel at 1000 W/m² irradiance level as measured on the solar simulator

4.3. I-V characteristics and maximum power produced as a function of operating temperature

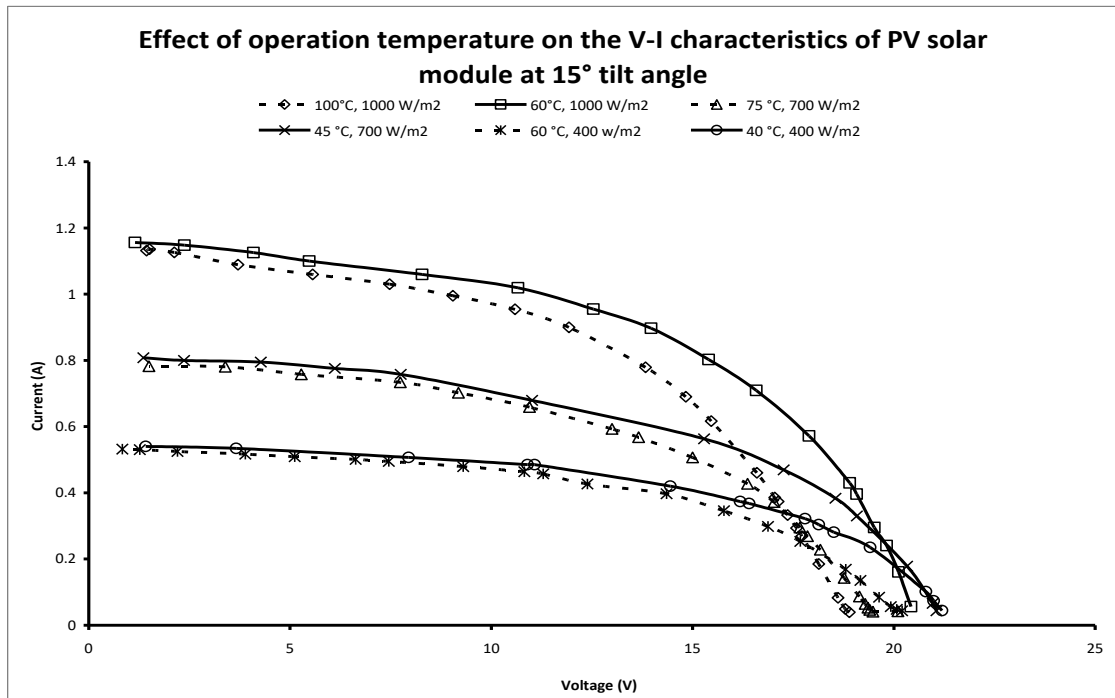


Figure 11 Effect of operation temperature on the V-I characteristics of PV solar module at 15° tilt angle as measured on the solar simulator

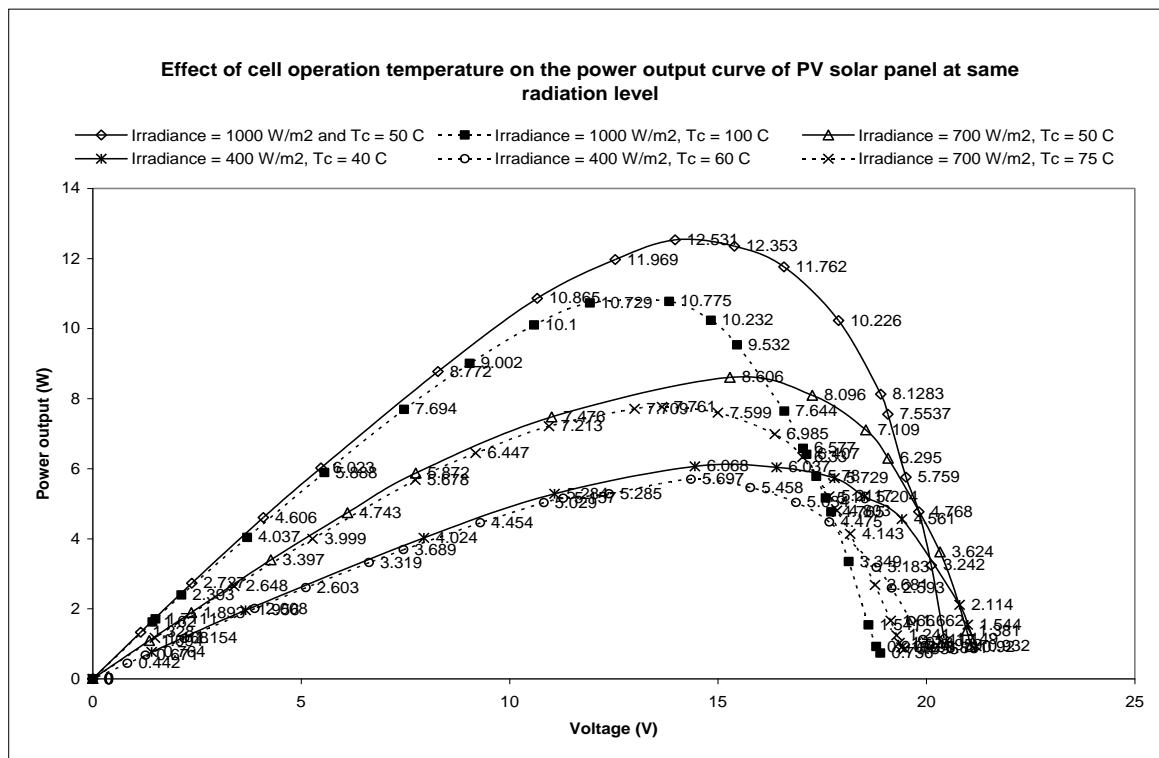


Figure 12 Effect of cell operation temperature on the power output of the PV panel at the same irradiance level at 15° tilt angle as measured on the solar simulator

It is known that the cell/module operation temperature (T_c) has some bearing on the V-I characteristics and maximum power output (P_{mp}) of the solar cell/module. In order to exactly quantify the effect of operating temperature on P_{mp} at the same radiation level and fixed tilt angle (15° with horizontal) for an amorphous silicon solar PV module, experiments were performed on a solar simulator to determine the V-I characteristics by varying the module operating temperature from 40°C to 100°C (Fig. 11). The power conditioning curves at the selected temperature range were also generated using the solar simulator and shown in Fig. 12. It was observed that at 1000 W/m^2 radiation level, P_{mp} increased by 14 % when panel temperature was lowered from 100°C to 60°C . At 700 W/m^2 radiation level, P_{mp} increased by 9.8% when panel temperature was lowered from 75°C to 45°C . Similarly, at 400 W/m^2 radiation level, P_{mp} increased by 6.1% when panel temperature was lowered from 60°C to 40°C . At other tilt angles of the panel, trend of V-I characteristic curves and P_{mp} were almost similar for the operating temperature range of 40°C to 100°C . Maximum power produced as a function of temperature for the solar module was also computed using Eq. 13 and compared with the experimental values generated using the solar simulator and mathematically computed values using Newton-Raphson’s iteration method. These values were slightly higher than the measured values but matched well with the mathematically computed values. The deviation from experimental values was due to the 18 % power degradation of the P_{mp} from the P_{initial} as suggested by Yamawaki et al., 2001 for amorphous silicon with use ($P_{mp} = 0.82 P_{\text{initial}}$).

4.4. Maximum power produced by the PV panel as a function of maximum swing angle of the sun away from the normal

4.4.1. Roof mounted inclinations of the panel

Maximum swing angle of the sun away from the normal position of the panel (λ) is computed and used in this study. It is very important parameter for computing the maximum power produced at noon during different months of the year at various latitudes. It is shown in Table 1 that for a polar mounted inclination of the panel, representative value of λ for the month of January (15th date) is around 21° for all the selected latitudes. The simulated study shows that for the selected range of irradiance (400 W/m^2 , 700 W/m^2 and 1000 W/m^2) when λ is 15° , P_{mp} is 9.23% less and when λ is 30° , P_{mp} is 14.15% less as compared to P_{mp} when the panel inclination is at normal to the sun ($\lambda = 0^\circ$). So, at $\lambda = 21^\circ$, P_{mp} produced would be around 11% less as compared to the P_{mp} produced at normal position of the panel. During February and August, the value of λ is around 13° and the equivalent loss in P_{mp} is around 9%. In the month of March and September, the value of λ is less than 3° (very small), which means the sun rays would strike the panel at almost normal position during the noon hours; there would be almost no loss of P_{mp} . In April and October, λ increases to about $9\text{--}10^\circ$ and its equivalent P_{mp} loss is about 6%. In May, λ further increases to about 18° and its equivalent P_{mp} loss in this month is about 10%. The maximum loss of P_{mp} occurs in the months of June and December when the λ increases above 23° and the equivalent loss in P_{mp} produced is about 12% as compared to the P_{mp} produced at normal position of the panel ($\lambda = 0^\circ$). The average λ for all the six winter months ($\bar{\lambda}_w$) and summer months ($\bar{\lambda}_s$) is computed using Eq. 17 and Eq. 18 show the annual loss of power which comes out to around 10 % at all the selected latitudes.

Table 2 Variation of maximum altitude angle of the sun and maximum swing angle of the sun at selected latitudes during all months of the year for winter and summer maximization panel inclinations

Month and date	20°N		30°N		40°N		50°N	
	α_s	λ	α_s	λ	α_s	λ	α_s	λ
January 15	48.67	06.33	38.68	06.32	28.68	06.32	18.66	06.34
February 15	56.82	01.82	46.80	01.80	36.80	01.80	26.74	01.74
March 15	67.37	12.37	57.35	12.35	47.30	12.30	37.30	12.30
April 15	79.11	05.89	69.23	05.77	59.20	05.80	49.20	05.80
May 15	87.44	02.44	78.81	03.81	68.91	03.91	58.87	03.87
June 15	86.37	01.37	83.21	08.21	73.13	08.13	63.25	08.25
July 15	87.44	02.44	81.11	06.11	71.26	06.26	61.28	06.28
August 15	83.21	01.79	73.33	01.67	63.38	01.62	53.41	01.59
September 15	71.62	13.38	62.13	12.87	51.72	13.28	41.68	13.32
October 15	59.99	01.99	49.90	04.90	39.94	04.94	29.67	04.67
November 15	47.14	07.86	40.69	04.31	30.66	04.34	20.67	04.33
December 15	46.55	08.45	36.51	08.49	26.49	08.51	16.44	08.56

It can thus be summarized that, If the panel is fixed at polar mounted inclination (facing south direction in northern hemisphere), the monthly loss of P_{mp} varies from 0 to 12% with annual loss of about 10% due to the movement of the sun away from the normal position during the noon hours at all latitudes.

For winter and summer maximization inclinations of the solar panel (Table 2), representative value of λ for the months of January and April is around 6° for all the selected latitudes and the equivalent loss of P_{mp} is less than 4% as compared to when λ is 0° . In February, λ is even less than 2° which shows that almost no loss of P_{mp} during the noon hours. However, in March λ increases above 12° which means about 8% loss of P_{mp} as compared to P_{mp} produced at normal position of the panel ($\lambda = 0^\circ$). There is a slight variation of λ at 20° N latitude as compared to 30 , 40 and 50° latitudes. At 30° and above latitudes, λ varies between 3 to 12° indicating a loss of P_{mp} between 1-7% only. The average λ for all the six winter months ($\bar{\lambda}_w$) and summer months ($\bar{\lambda}_s$) is also computed to show the seasonal loss of power which comes out to be not more than 6% at all latitudes. It shows that at the summer and winter maximization inclination of the panel, 4% more power is produced year round as compared to the polar mounted inclination of the panel.

4.4.2. South facing vertical wall mounted inclinations of the panel/thin films

For the solar PV panel/thin films mounted/fixed on the south facing vertical walls/windows, the sun will never be at the normal position of the panel surface. The maximum altitude angle of the sun at noon (α_s) will then be equal to the maximum swing angle of the sun during noon hours (λ). Table 1 shows that at 20° N latitude (near equator locations) the sun shines between 70° to 88° angle with horizontal (on the panel surface) after mid-March to mid-September during noon hours, indicating almost 75% of the solar radiation being reflected from the glass cover of the panel without being absorbed and very little P_{mp} being produced. Similarly, for the other months of the year (October – February) there is again a significant loss of P_{mp} (about 15% to 50%) as the variation of maximum swing angle λ is still on the higher side (around 36° to 60°). It is important to note that there is significant loss in maximum power produced when λ increases from 45° to 60° as indicated by the experimental study. It is due to the increase in reflection losses from the glass cover over the panel surface. At 60° inclination of the panel the maximum P_{mp} produced is about half its value as compared to its normal position. Similarly, at 30° N latitude, the maximum swing angle (λ) after mid-April to mid-August is between 70° and 83° , which means almost 70% the solar radiation would be reflected from the glass cover of the panel without being absorbed and very little P_{mp} is produced. However, during the other months of the year (September to March), λ varies between 36° and 60° indicating the loss in P_{mp} between 15% and 45%. However, at 40° N and 50° N latitudes, the maximum swing angle λ is nearly equal to 60° just for four and three summer months respectively. During this period the P_{mp} produced will be about half the value as compared to P_{mp} produced at normal position of the panel. For the other eight to nine months of the year, λ does not exceed 45° , indicating the maximum loss of P_{mp} to be not more than 20%. It can thus be summarized that at 20° and 30° N latitudes, during summer months (April-September) there is not much benefit of using the south facing vertical walls/windows for fixing of solar panels/thin films for generating electricity. During the other months there is an about 30% to 50% more area requirement for producing the same P_{mp} as compared to the P_{mp} produced using roof top mounted optimum inclinations. However, at 40° and 50° N latitudes, only three to four summer months would not be as effective but during the other eight to nine months just 15% to 25% more area would be required on the vertical walls to produce the same amount of P_{mp} as compared to the roof top mounted inclinations of the solar PV panels.

4.5. Validation of the proposed mathematical model

A comparison of the measured values of maximum power produced ($P_{mp(m)}$) using solar simulator the computed values of maximum power produced ($P_{mp(c)}$) (using mathematical computations) at various selected irradiance levels and tilt angles of the panel is shown Fig.13. It is clearly indicated that these values match well within less than 5% deviation. It is also observed that the P_{mp} decreased gradually with the increase in the tilt angle. However at 60° inclination of the panel, there is sudden drop in P_{mp} produced.

The measured and computed values of P_{mp} at various selected irradiance level (at horizontal position of the panel, $\lambda = 0^\circ$) are shown in Fig. 14 which clearly indicate that there is complete matching of the two set of values within less than 4% deviation, thus again proving the accuracy of the developed model.

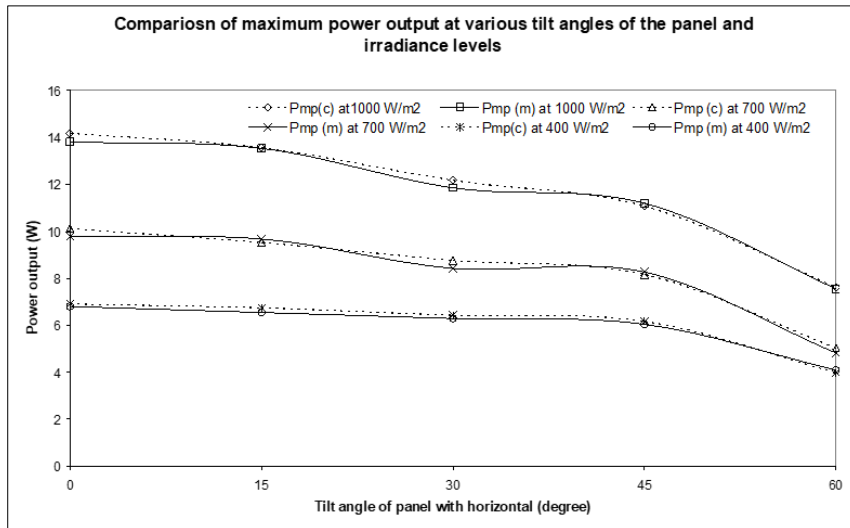


Figure 13A comparison of computed and measured values of maximum power produced at various tilt angles and irradiance levels

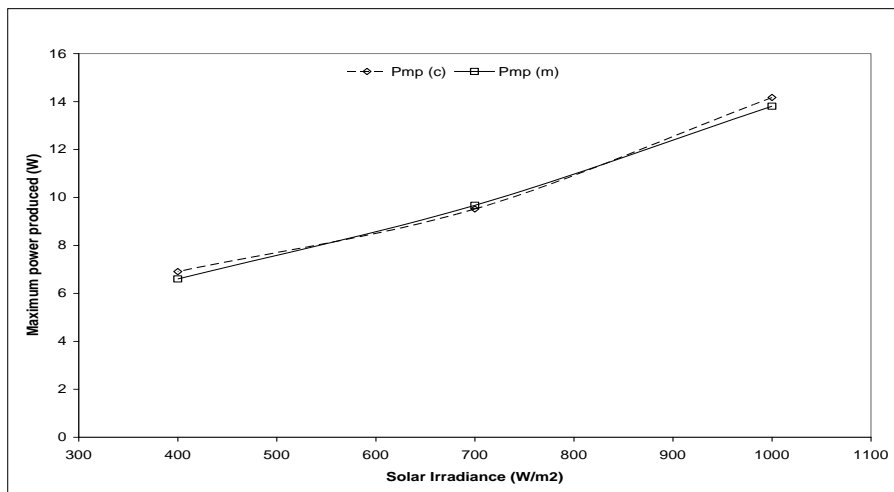


Figure 14A comparison of computed and measured values of maximum power produced at various selected irradiance levels at normal position of the panel ($\lambda = 0^\circ$)

Nomenclature

- E : Irradiance, $W\ m^{-2}$
- P_{mp} : maximum power produced, W_p
- V_{mp} : voltage at maximum power point, V
- I_{mp} : current at maximum power point, A
- FF : fill factor
- V_{oc} : open circuit voltage, V
- I_{sc} : short circuit current, A
- η_c : electrical efficiency, %
- η_{Tref} : module's electrical efficiency at the reference temperature, %
- G_T : solar radiation flux, $W\ m^{-2}$
- β_{ref} : temperature coefficient, K^{-1}
- T_c : panel operation temperature, $^\circ C$
- γ : solar radiation coefficient

I :	current at any point on the I-V curve, A
I_{il} :	electric current generated by illumination, A
I_o :	diode current, A
R_s :	inner resistance, Ω
V_T :	Thermal voltage, V
M :	diode factor
Q :	electron charge ($= 1.602 \times 10^{-19}$ C)
K :	boltzmann constant ($= 1.38 \times 10^{-23}$), J K ⁻¹
λ :	maximum swing angle of the sun away from the normal position of the panel, ($^\circ$)
ϕ :	latitude of a place, ($^\circ$)
α_s :	maximum angle of the sun at noon, ($^\circ$)
λ_w :	average swing angle of the sun away from the normal for winter months, ($^\circ$)
λ_s :	average swing angle of the sun away from the normal for summer months, ($^\circ$)
ω :	hour angle of the sun, ($^\circ$)
δ :	declination angle of the sun, ($^\circ$)
N :	day of the year starting from Jan 1

5. Conclusion

- As the cell/panel operation temperature decreases, the electrical efficiency of the panel increases.
- 2. At the same operation temperature, electrical efficiency increases with increase in solar irradiance.
- The effect of increase in the cell/module operation temperature (T_c) on the maximum power produced at noon (P_{mp}) shows that when the T_c is lowered from 100°C to 50°C, 14 % increase in P_{mp} is observed at 1000 W/m² irradiance level.
- Maximum swing angle of the sun away from the normal position of the panel (λ) computed in this study is a very important parameter for computing the maximum power produced at noon (P_{mp}) during different months of the year at various latitudes.
- There is about 9% to 19% drop in the maximum power produced (P_{mp}) by the panel when λ varies between 15° and 45° as compared to the P_{mp} produced at $\lambda = 0^\circ$. However at $\lambda = 60^\circ$, P_{mp} produced is about half the value as compared to the P_{mp} produced at $\lambda = 0^\circ$.
- For a panel fixed at polar mounted inclinations (facing south direction in northern hemisphere), the monthly loss of P_{mp} varies from 0 to 12% during different months of the year with an average annual loss of P_{mp} equal to 10% due to the movement of the sun away from the normal position during the noon hours at all latitudes.
- For a panel mounted at the summer and winter maximization inclinations, about 4% more P_{mp} is produced year round as compared to the polar mounted inclinations of the panel at all latitudes.
- For the solar PV panel/thin films mounted/ fixed on the south facing vertical walls/windows at 20° and 30°N latitudes during the summer months, P_{mp} produced during noon hours is even less than half the P_{mp} produced by the panel at the polar mounted inclination. Also, during the other months of the year, 50% to 35% more area requirements on the south facing vertical walls are needed to produce the same P_{mp} if the panel is fixed on the polar mounted inclination on the south facing roof.
- At 40° and 50°N latitudes, during the eight to nine months of the year (except the three summer months), variation in λ is not more than 45°, indicating the maximum loss of P_{mp} to be not more than about 20%, which means about 25% to 15% more wall area is required on the vertical walls to produce the same amount of P_{mp} as compared to the polar mounted inclinations of the solar PV panels.
- The measured and computed values (using mathematical iterations) of maximum power produced at various selected irradiance levels and tilt angles of the panel match well within less than 5% deviation thus proving the accuracy of the developed model

Compliance with ethical standards

Acknowledgments

The authors are thankful to the Head, Department of Computer Sciences and Electronics and the Head, Department of Mechanical Engineering, North Dakota State University, Fargo, USA for providing all the laboratory facilities and the necessary material and instruments for conducting very useful study on solar PV panels. The cooperation of all the technical and office staff from both the laboratories and departments is also acknowledged.

References

- [1] Abdulmunem R. A, Pakharuddin M S, Hasimah AR, Hashim AH, Habibah G. (2021) Numerical and experimental analysis of the tilt angle's effects on the characteristics of the melting process of PCM-based as PV cell's backside heat sink. *Renewable Energy* 173, 520-530
- [2] Balenzategui, J., Chenlo, F., 2005. Measurement and analysis of angular response of bare and encapsulated silicon solar cells. *Solar Energy Materials & Solar Cells* 86, 53–83.
- [3] Cheng, C.L., Jimenez, C.S.S., Lee, M.-C., 2009. Research of BIPV optimal tilted angle, use of latitude concept for south orientated plans. *Renewable Energy* 34, 1644–1650.
- [4] Elsayed, M.M., 1989. Optimum orientation of absorber plates. *Solar Energy* 42, 89–102.
- [5] EL-Kassaby, M.M., 1988. Monthly and daily optimum tilt angle for south facing solar collectors; theoretical model, experimental and empirical correlations. *Solar & Wind Technology* 5, 589–596.
- [6] Friedman, 1996, Friedman, D.J., 1996. Modelling of tandem cell temperature coefficients. In: *Proceedings of 25th IEEE PVSC*, 89.
- [7] Green, M.A., Emery, K., Blakers, A.W., 1982. Silicon solar cells with reduced temperature sensitivity. *Electron. Lett.* 18, 97.
- [8] Gunerhan, H., Hepbasli, A., 2007. Determination of the optimum tilt angle of solar collectors for building applications. *Building and Environment* 42, 779–783.
- [9] Hussein, H.E.-G.H.M.S., Ahmad, G.E., 2004. Performance evaluation of photovoltaic modules at different tilt angles and orientations. *Energy Conversion and Management* 45, 2441–2452.
- [10] Jacobson MZ and Jadhav Vijaysinh (2018). World estimates of PV optimal tilt angles and ratios of sunlight incident upon tilted and tracked PV panels relative to horizontal panels. *Solar Energy* 21, 55-66.
- [11] Kaddoura TO, Ramli MAM, Al-Turki YA (2016). On the estimation of the optimum tilt angle of PV panel in Saudi Arabia. *Renewable and Sustainable Energy Reviews* 65, 626-634.
- [12] Lewis, G., 1987. Optimum tilt of a solar collector. *Solar & Wind Technology* 4, 407–410.
- [13] Ibrahim, D., 1995. Optimum tilt angle for solar collectors used in cyprus. *Renewable Energy* 6, 813–819.
- [14] Mamun M.A.A, Hasanuzzaman M.M.M Islam, Jeyraj Selvaraj (2021). Effect of tilt angle on the performance and electrical parameters of a PV module: Comparative indoor and outdoor experimental investigation. *Energy and Built Environment*. In press, corrected proof. Available online 2 March 2021.
- [15] Meng B, Loonen R.C.G.M, Hensen J.L.M. (2020). Data-driven inference of unknown tilt and azimuth of distributed PV systems. *Solar Energy* 211, 418-432.
- [16] Nakamura, H., Yamada, T., Sugiura, T., Sakuta, K., Kurokawa, K., 2001. Data analysis on solar irradiance and performance characteristics of solar modules with a test facility of various tilted angles and directions. *Solar Energy Materials & Solar Cells* 67, 591–600.
- [17] Nann and Emery, 1992, Nann, S., Emery, K., 1992. *Sol. Energy Mater. Sol. Cells* 27, 189.
- [18] Notton, G., Cristofari, C., Mattei, M., Poggi, P., 2005. Modelling of a double-glass photovoltaic module using finite differences. *Applied Thermal Engineering* 25, 2854–2877.
- [19] Osterwald, C.R., Glatfelter, T., Burdick, J., 1987. Comparison of the temperature coefficients of the basic I–V parameters for various types of solar cells. In: *Proceedings of 19th IEEE PVSC*, 188.
- [20] Ruidong Xu, Kai Ni, Yihua Hu, Jikai Si, Huiqing Wen, Dongsheng Yu (2017). Analysis of the optimum tilt angle for a soiled PV panel. *Energy Conversion and Management* 148, 100-109.
- [21] Sethi, V.P. 2009. On the selection of shape and orientation of a greenhouse: thermal modeling and experimental validation. *Solar Energy* 83 (1), 21-38.
- [22] Skoplaki, E., Palyvos, J.A., 2009. On the temperature dependence of photovoltaic module electrical performance: A review of efficiency/power correlations. *Solar Energy* 83, 614-624.
- [23] Soulayman, S.S., 1991. On the optimum tilt of solar absorber plates. *Renewable Energy* 1, 551–554.
- [24] Sze, S.M., 1981. *Physics of Semiconductor Devices*, second ed. John Wiley and Sons, New York. pp. 79–807.

- [25] Ullah A, Imran H, Maqsood Z, Butt NZ (2019). Investigation of optimal tilt angles and effects of soiling on PV energy production in Pakistan. *Renewable Energy*. 139, 830-843.
- [26] Villalva, M.G., Gazoli, J.R., Filho, E.R., 2009. Comprehensive approach to modeling and simulation of photovoltaic arrays. *IEEE Transactions on power Electronics* 24, 1198-1208.
- [27] Wagner, A., 2006. *Photovoltaic Engineering*, zweite ed. Springer, Berlin, Heidelberg.
- [28] Wysocki, J.J., Rappaport, P., 1960. Effect of temperature on photovoltaic solar energy conversion. *J. Appl. Phys.* 31, 571–577.
- [29] Yadav Somil and Panda S.K. (2020). Thermal performance of BIPV system by considering periodic nature of insolation and optimum tilt-angle of PV panel. *Renewable Energy* 150, 136-146.
- [30] Yamawaki, T., Mizukami, S., masui, T., Takahashi, H., 2001. Experimental investigation on generated power of amorphous PV module for roof azimuth. *Solar Energy Materials and Solar Cells* 67, 369-377
- [31] Zondag, H.A., 2007. Flat-plate PV-thermal collectors and systems – a review. *Renew. Sustain. Energy Rev.* doi:10.1016/j.rser.2005.12.012